Light Metals 2013 *Edited by: Barry Sadler*
TMS (The Minerals, Metals & Materials Society), 2013

INFLUENCE OF VANADIUM ON THE MICROSTRUCTURE OF A356 FOUNDRY ALLOY

Thomas H. Ludwig[1], Paul L. Schaffer[2], Lars Arnberg[1]
[1]Norwegian University of Science and Technology, Alfred Getz Vei 2, Trondheim, 7491, Norway
[2]Hydro Aluminium, Research and Technology Development, Romsdalsvegen 1, Sunndalssøra, 6601, Norway

Keywords: Vanadium, Al-Si alloy, Al-Si-V system, Grain refinement, A356 alloy

Abstract

Increasing vanadium content in coke used for anodes in aluminium production will lead to rising vanadium concentrations in primary aluminium. Consequently, the vanadium will be found in downstream products such as foundry alloys at levels well above current alloy specifications. The work presented in this article focuses on the effect of different vanadium concentrations on the microstructural features of an as-cast A356 alloy. It is shown that vanadium in excess of 0.2 wt% cause crystals with a distinct polyhedral morphology to precipitate. This phase was identified as Si_2V by SEM-EDS measurements. Moreover, traces of vanadium were found in the β-Al_5FeSi phase. When the vanadium concentration was increased from 0.06 to 0.8 wt% gradual vanadium enrichment of the β-Al_5FeSi from 0.4 to 5.9 wt% occurred. Iron rich particles, which had some solubility for vanadium possessed an almost globular shape and were located within α-Al dendrites or close to the dendrite/eutectic interface.

Introduction

Recent publications have shown that it is primarily the fluctuation and the decline in raw material quality that leads to higher trace element contamination of pot line aluminium [1]. The main source for pick up of the element V during the electrolytic reduction of alumina to primary aluminium is the petroleum coke used in the anodes. Minor contributions come from the alumina. The wide span of V concentrations arises in particular from the grade of crude oil which is used for the production of calcined petroleum coke. Jha et al. [2] reported fluctuations between 220 and 1500 ppm V in the calcined coke. As a result V concentrations are expected to increase in primary Al and eventually find their way into the end products of wrought and foundry alloys. Grandfield et al. [3] comment that some wrought alloys have upper V concentration limits of 500 ppm, while electrical grade aluminium may only allow 100 ppm V. For foundry alloys, V specifications are normally listed within the column "Others" with typical concentrations each < 0.01 wt% and total maximum concentration of 0.15 wt% without defining a clear limiting value. These specifications are expected to be displaced to higher V concentration. Following the remarks of Grandfield et al., the predicted increase of V in primary alloys will soon result in concentrations exceeding 150 ppm. As a consequence, it is important to investigate the effect of higher V contents on the microstructure and solidification of an industrially important foundry alloy, A356, of the Al-Si alloy series.

Experimental

Commercial A356 foundry alloy was used as the base metal in the present investigation. The chemical composition is summarized in Table 1. Vanadium was added to the melts in the form of waffle ingot material of Al-10 wt pct V master alloy. In addition to Al and V, the master alloy contained 0.3 wt% Si and Fe, while other impurities were specified as < 0.1 wt%. The nominal V additions were 0.06, 0.2, 0.5 and 0.8 wt%. Melts for thermal analysis investigations and for sampling of specimen for microscopy studies were produced by melting of approximately 1kg charge material at 750 °C in a boron-nitride coated clay-graphite crucible in a resistance furnace. After the addition of the master alloys the melts were stirred and allowed to settle for 30 min to ensure complete dissolution of the Al-V master alloy.

Table I Chemical composition of the A356 foundry alloy in wt%

Al	Si	V	Zn	Fe	Mg	Mn
Bal.	7.22	0.0064	0.003	0.09	0.31	0.006

The experimental setup for thermal analysis measurements is depicted in Fig. 1. A graphite crucible was preheated at 760 °C and placed on top of the skimmed and thoroughly stirred melt. After the temperatures of crucible and melt had reached equilibrium, samples were taken by submerging the graphite crucibles into the melt. The filled crucibles were then placed on Fiberfrax board and a K-type thermocouple was lowered into the melt. The thermocouple tip was positioned 10 mm from the bottom and centered in the sample. A Campbell logger (Campbell Scientific, Inc., USA) recorded the temperature-time curve at a frequency of 50 Hz. In the course of data processing, this oversampling was averaged to yield a frequency of 10 Hz. Prior to and after a measurement the range of eventual thermocouple drift was checked against high purity aluminum (A15N grade) assuming a solidus temperature of 660 °C. This experimental setup gives a solidification rate of 1.1 K/s.

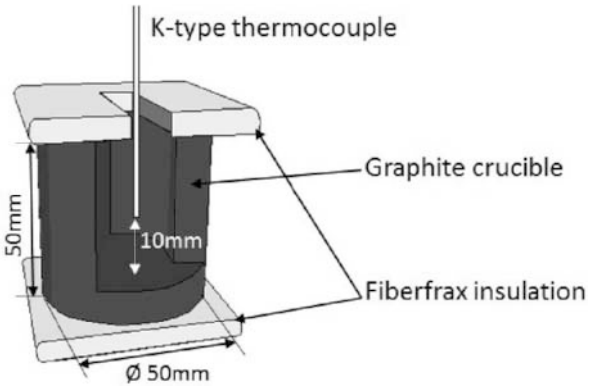

Figure 1 Schematically illustration of the thermal analysis setup used in the present investigations.

Temperatures characteristic for the nucleation and growth of the α–Al were determined by applying the method of Tamminen. For a more detailed description of the analysis technique the reader is referred to the corresponding literature [4]. The TAW32 software [5] was used to compare the first derivative dT/dt curve with the

idealized curve of zero latent heat release to define the nucleation temperature of α–Al $T_{N,\alpha}$. Analysis of the cooling curve provided the minimum temperature $T_{min,\alpha}$, the growth temperature $T_{G,\alpha}$ and the recalesence undercooling $\Delta T_{R,\alpha}$ ($\Delta T_{R,\alpha} = T_{G,\alpha} - T_{min,\alpha}$) of the α–Al reaction.

For microscopy studies, samples were produced in the same way as described above, however no thermocouple was placed in the filled graphite crucibles. The cylindrical samples with the following dimensions; diameter of 30 mm and 40 mm in height, were sectioned vertically along their center line. Cold embedding with subsequent grinding and polishing was carried out in accordance with standard metallographic sample preparation. The last step was a finishing step with active colloidal silica suspension. Samples for grain size measurements were additionally anodized with a solution of H_2O and 5 % HBF_4 (by volume). Subsequently, light micrographs were taken with a Leica MEF4M optical microscope (Leica Microsystems GmbH, Germany) equipped with digital image aquisition at 25x magnification and the grain size was measured according to the linear-intercept method (ASTM E112) with a dedicated tool of the image analysis software ImageAccess (Imagic AG, Switzerland).

Scanning electron microscopy (SEM) and energy-dispersive X-ray spectroscopy (EDS) studies were performed on a LV-SEM Zeiss Supra 55 VP (Carl Zeiss Microscopy GmbH, Germany) equipped with an EDAX Genesis EDS system (EDAX Inc., USA), and on a Hitachi SEM S-3400N (Hitachi Europe GmbH, Germany) equipped with a INCAEnergy EDS system (Oxford Instruments, UK).

FactSage™ 6.1 and the FactLite database was used for thermodynamic calculations in the ternary Al-Si-V system and the results were compared to existing literature on multicomponent phase diagrams [6-8].

Results

Temperature Characteristics and Grain Size

Table II summarizes the results from the analysis of cooling curves and first derivate obtained by thermal analysis measurements of the α–Al reaction. The reproducibility of these temperatures was in the range of ± 0.25 K within one series of experiments. Each temperature is the average of at least 3 repeated measurements. The results reveal a clear trend where the nucleation temperature of primary aluminium as well as growth of the aluminum dendrites shifts to a higher temperature with increasing V. For the highest V addition of 0.8 wt% this constitutes a 4 K temperature increase. The recalesence undercooling of the α–Al reaction was only slightly affected. It dropped by up to 0.5 K for the 0.2 wt% V addition, but rose to the same values similar to temperatures obtained with the reference alloy.

Table II Characteristic temperatures for nucleation and growth of the α-Al phase

V conc. wt%	$\mathbf{T_{N,\alpha}}$ °C	$\mathbf{T_{min,\alpha}}$ °C	$\mathbf{T_{G,\alpha}}$ °C	$\mathbf{\Delta T_{R,\alpha}}$ K
reference	612.2	610.3	612.0	1.7
0.06	612.6	611.6	612.9	1.3
0.2	613.8	612.4	613.6	1.2
0.5	614.4	612.4	614.2	1.8
0.8	615.9	614.1	615.6	1.5

An average of 8 micrographs taken from areas in the vicinity of the thermocouple tip of anodized samples has been measured by means of the linear-intercept method, to gather statistically relevant data for the grain size in alloys with increasing V concentration. The results are shown in Fig. 2. With the majority of the results lying within a narrow band between 200 and 250 µm in average equivalent diameter, it appears to be difficult to define a clear trend. The grains seem to become smaller, by increasing the V concentration. At 0.8 wt% V, however, the values start to rise again and the data scatters noticeably.

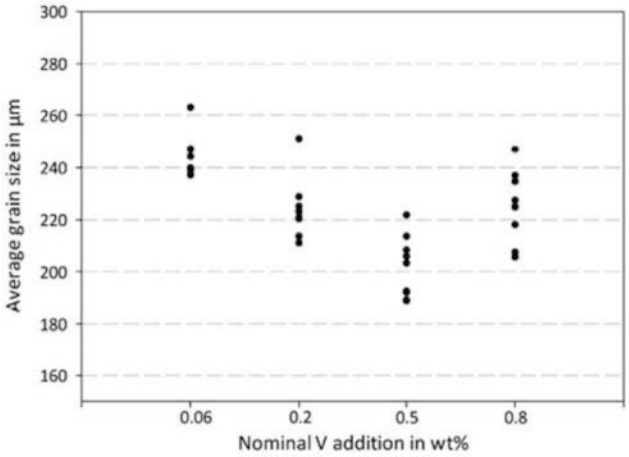

Figure 2 Correlation of α-Al grain size and V concentration. Each data point represents the average grain size of grains in one corresponding micrograph.

Microstructure and Composition of V-rich phase

In Fig. 3 the typical microstructural features of an as cast A356 with 0.2 wt% V addition are shown. In addition to the two phases which are pointed out in the micrograph (i.e. Si_2V and β-Al_5FeSi), dendritic Al, flake-like eutectic Si (dark grey) and α-$Al_8Mg_3FeSi_6$ (brighter grey) in an array of morphologies (compact blocky, Chinese script and needle-like) were present. Vanadium rich particles possessed a distinct polyhedral morphology. These particles were frequently observed to be heavily fractured as shown in Fig. 4(b). The size was typically in the range of 8 to 35 µm in equivalent diameter. They were generally found close to the aluminium dendrite tips as pointed out in Fig. 3 or within the α–Al grains. A V concentration of 0.2 wt% was the lowest concentration for Si_2V to be identified in the microstructure of the A356 alloy.

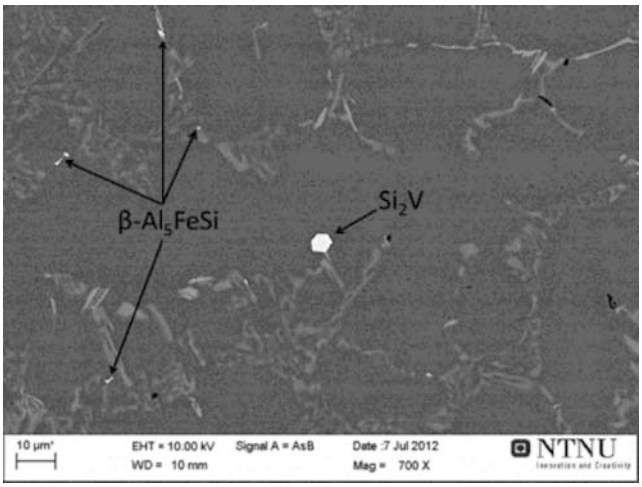

Figure 3 SEM micrograph (backscattered mode) of the as cast microstructure of A356 with 0.2 wt% V. The contrast-brightness balance has been adjusted for clarification in favor of the heavier element containing phases.

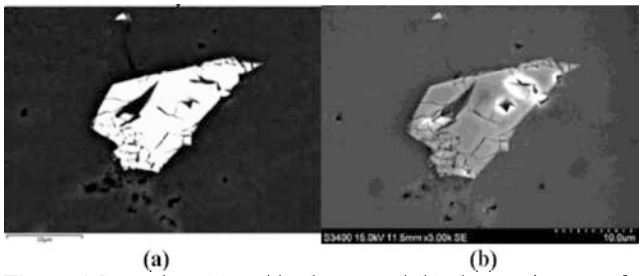

Figure 4 Secondary (a) and backscattered (b) electron images of a Si_2V particle with a distinct polyhedral morphology located with the α–Al phase in a sample with 0.5 wt% V.

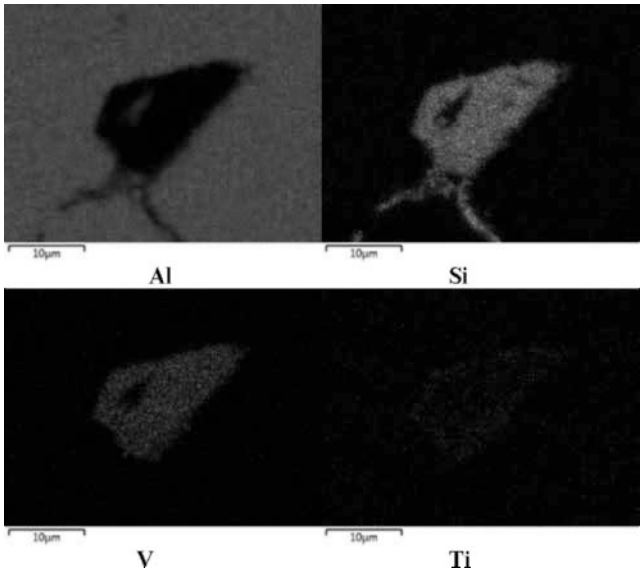

Figure 5 Corresponding SEM-EDS element map of the particle shown in Fig. 3.

In order to eventually indentify the V-rich particles as Si_2V, several particles with similar morphology were investigated with EDS element mapping and spot analysis. The results are presented in Fig. 5 and 6, respectively. The semi quantitative mappings show strong counts for Si and V as well as for Ti, which was encountered in almost every V-rich particle. Conclusive proof of the phase being Si_2V was achieved with the EDS spot measurements. A representative reading is given for the particle depicted in Fig. 4. The particles Si:V at% ratio was close to the theoretical one which is 2:1.

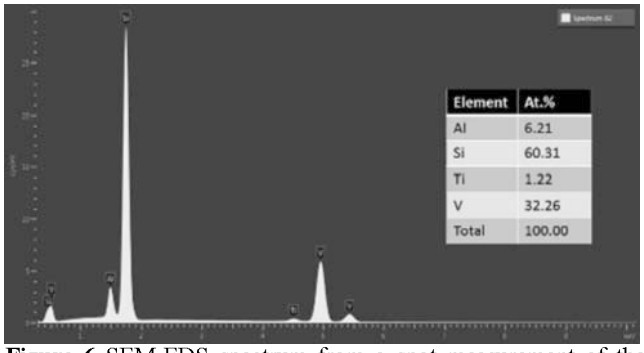

Figure 6 SEM-EDS spectrum from a spot measurement of the polyhedral crystal in Fig. 3 confirms the presence of Si_2V.

Microstructure and Composition Fe-rich phase

In contrast to V free A356 alloy and alloys with V addition of 0.06 wt% where the β-phase mainly takes on a needle-like shape, the β-Al_5FeSi phase was predominantly present in a globular or/and rounded flake morphology. A representative SEM micrograph of a globular β-Al_5FeSi is shown in Fig. 7. Globular β-phase particles were located close to dendritic regions and were surrounded by Mg_2Si, whereas rounded-flakes were connected to the α–phase ($Al_8Mg_3FeSi_6$) particles, which appeared in Chinese script or in more compact blocky form. Some of the β-phase particles were further investigated by EDS. The resultant EDS spectrum of the particle in Fig. 7 is shown in Fig. 8. Peak signals inherent for V were obtained. The Al:Fe:Si at% ratio of 70:14:14 was as demonstrated for the representative particle, also attained for other Fe-rich particles. This is close to the ideal at% ratio of β-Al_5FeSi with typical Fe:Si at% ratios ranging from 1:1 to 1:1:3.

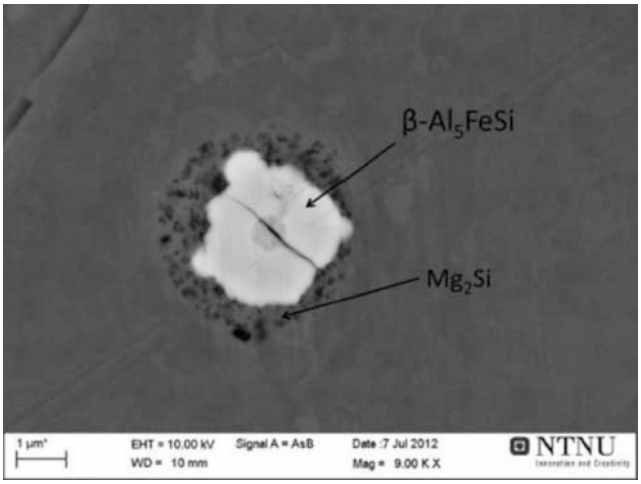

Figure 7 SEM micrograph (backscattered mode) of an as-cast A356 sample alloyed with 0.8 wt% V featuring a globular β-Al_5FeSi particle.

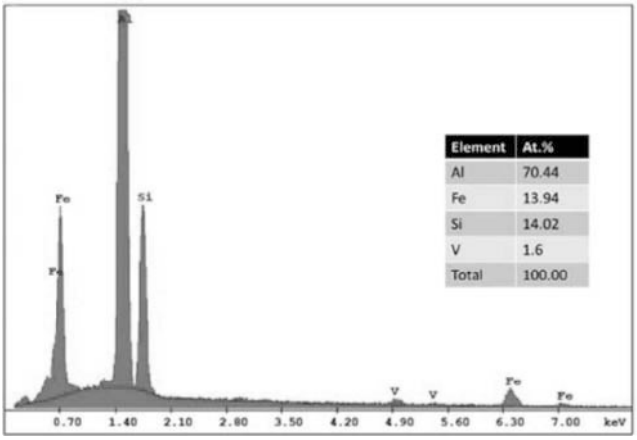

Figure 8 SEM-EDS spectrum from a spot measurement of the globular particle in Fig. 6 confirms the V enrichment of the β-Al_5FeSi phase.

The results in Fig. 9 document a gradual V enrichment in the β-Al_5FeSi phase with increasing nominal V additions to the melt. The data plotted here was obtained by measuring a statistically significant number of particles by EDS. When 0.06 wt% was added, only a few β- phase particles showed weak counts for V, mostly in Fe layers on eutectic Si crystals. This changed as the V concentration was increased to 0.8 wt%. Peak values of up to ~6 wt% V were measured in the globular β-Al_5FeSi particles.

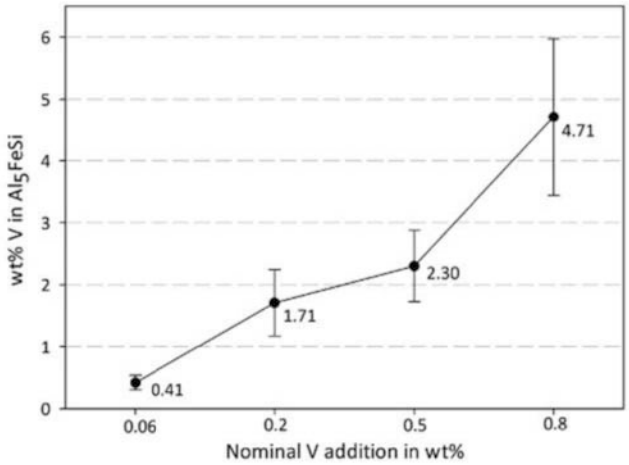

Figure 9 Relationship of overall V concentration and V content of the β-Al_5FeSi phase. The standard deviation σ is given as error bars.

Thermodynamic calculations

The liquidus projection of the Al-rich corner in the ternary Al-Si-V as calculated with FactSage™ between 540 and 800 °C in the composition range of the present investigations is shown in Fig. 10(a). An enlargement of the liquidus projection in the region of the ternary eutectic point (Liq. → Al(s) + Si(s) + Si_2V(s)) is shown in Fig. 10(b). Isotherms are plotted as dotted lines, whereas straight lines show the eutectic valleys. The primary crystallization fields of Al_3V, $Al_{23}V_4$, Al_7V, $Al_{10}V$ (in order of formation), Al, Si and Si_2V are outlined. The main liquidus line intersects a number of peritectic points in the sequence of the Al-V compounds until the ternary eutectic point at 573.4 °C is reached. From this liquidus projection it is shown that primary crystallization of an alloy with 7 wt% Si occurs in the phase field of Si_2V when the V concentration exceeds 0.06 wt%. Corresponding vertical sections for 0.06 and 0.8 wt% V with the V concentration being the fixed value are given in Fig. 10 (c) and (d). The vertical section for 0.06 wt% V underlines that Al is the first phase to form. It also predicts a narrow temperature window of simultaneous formation of Al and Si_2V (Liq. + Al → Liq. + Al + Si_2V) that due to compositional changes during solidification is not likely to be crossed. In contrast, with nominal V concentrations ranging between 0.2 and 0.8 wt% Si_2V solidifies first. Upon further cooling and while the solute concentrations in the liquid changes, the general increase in V concentration displaces in particular the reaction of Liq. → Liq. + Si_2V and consequently also the theoretical line of the reaction Liq. + Si_2V → Liq. + Al + Si_2V to higher temperatures as shown by the sequence of isopleths in Fig. 10 (c) and (d) and in the liquidus projection. The resulting change of the formation temperatures for α–Al were calculated, summarized and compared to the nucleation temperatures of α–Al obtained from thermal analysis in Table III. For the idealized case of a ternary Al-Si-V system assuming equilibrium conditions, the same trend of increasing temperatures was found. The FactSage™ calculations predicted a ~5K increase when the V concentration was increased to 0.8 wt%. It should be noted that the predicted formation temperature of α–Al is up to 7 K higher compared to the experimental data.

Table III Comparison of temperature of formation of α–Al obtained by thermodynamic calculations and experiments.

	V concentration in wt%				
Temperature (°C)	Ref.	0.06	0.2	0.5	0.8
FactSage™	617.0	617.8	618.7	620.7	622.6
Experiment	612.2	612.6	613.8	614.4	615.9

Discussion

According to Mondolfo [9] V has a mild grain refinement effect, but compared to conventional grain refiners such as Ti and TiB_2 vanadium is rather inefficient. The phase that comes into question to add to grain refinement effects is Al_3V which has an Al_3Ti-type crystal structure. Thus V could theoretically substitute for Ti and act as the coating layer on TiB_2 [10]. There is, however, considerable disagreement in the literature to what extent V plays a role as grain refiner. Edwards et al. [11] report a decrease of grain size in a near eutectic Al-Si piston alloy with a combined addition of Ti, Zr and V. Maitland [12] reports a slight grain refinement with V addition. This was most prominent for a combined addition of Mn and V in wrought AlMgSi alloys. Others deny any effect of V [13]. In the present study we cannot define a trend consistent with V additions. The grain size was rather stable with some scatter in a band between 200 and 250 µm. We argue that high Si concentration of 7 wt% as in the A356 alloy does not allow for the formation of Al_3V. Even if the Si concentration was lower (< 5 wt%) and the V content sufficiently high (> 0.5 wt%) to allow primary crystallization of Al_3V, it seems unlikely stable Al_3V particles would form, because solidification proceeds through a cascade of univariant reactions [7].

A polyhedral phase precipitated at V concentrations of > 0.2 wt%. This phase was indentified by its at% ratio as Si_2V. The particles

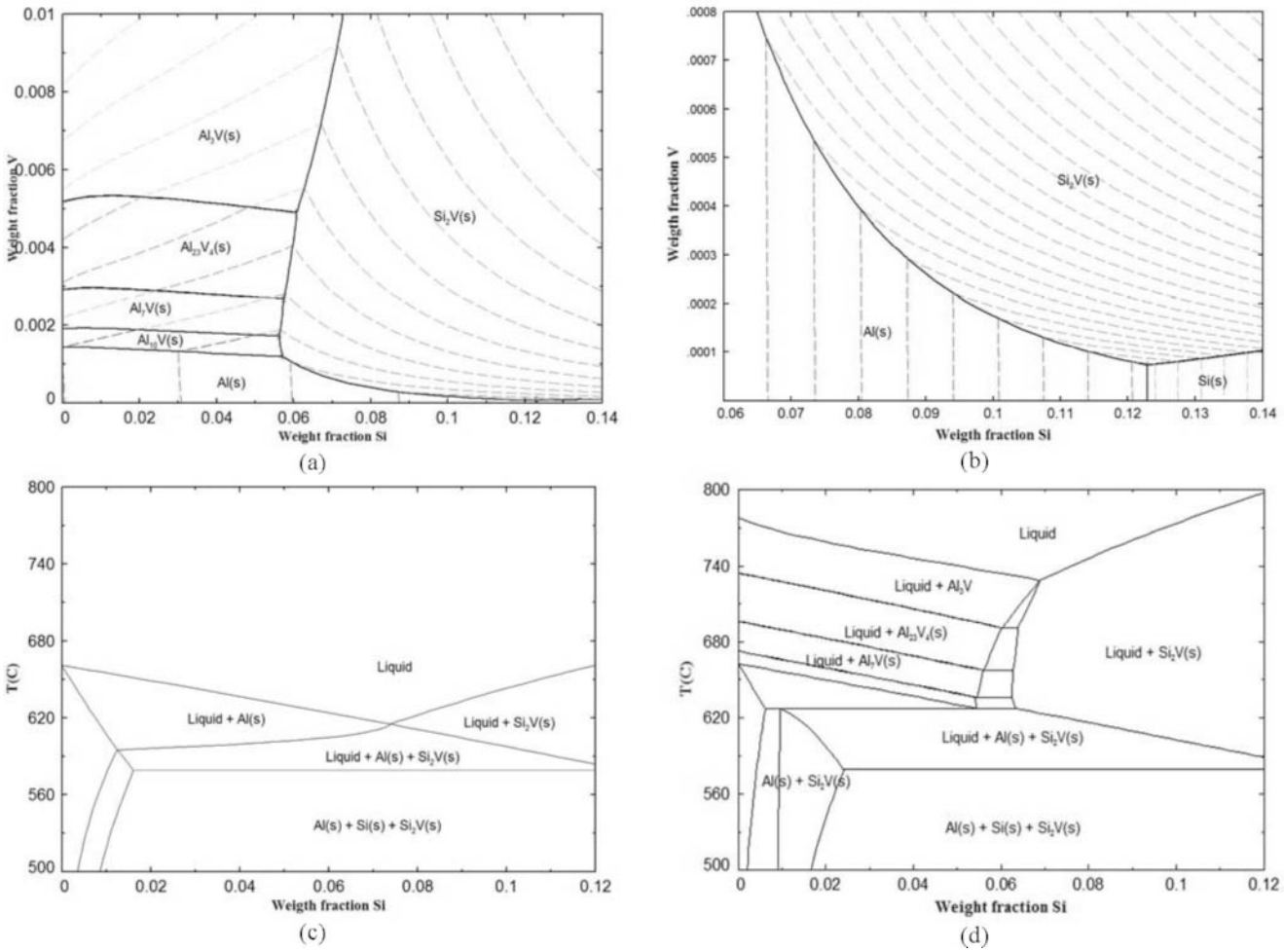

Figure 10 Liquidus projection of the Al-rich corner of the ternary Al-Si-V phase diagram (a); enlargement of the eutectic valley at the ternary eutectic point (b); and vertical sections at 0.06 wt% V (c) and 0.8 wt% V (d) calculated with FactSage^{TM}.

were located close to dendrite tips or within the Al-Si eutectic close to the dendrite-eutectic interface. This indicates that Si_2V nucleated and grew during the early stages of solidification and was pushed into the interdendritic spaces by the growing α–Al dendrites. Factsage^{TM} calculations confirm this. They predict primary crystallization of Si_2V for V concentration exceeding 0.06 wt% and primary crystallization of α–Al, given that solidification proceeds sufficiently slow to meet equilibrium condition as predicted in the FactSage^{TM} calculation. Furthermore, it was shown that a temperature window exists for simultaneous crystallization of α–Al and Si_2V, when the eutectic valley which slopes to the ternary eutectic point is reached. Phase diagram evaluations in the literature [6, 7] are in contradiction to the Factsage^{TM} calculations. They predict primary crystallization of α–Al for the Si content typical for an A356 alloy and V additions of up to 0.8 wt%. An example of a liquidus projection in the Al-rich corner of the ternary Al-Si-V diagram from the literature shown in Fig. 11 (note the phase composition is given in at%). However, experimentally obtained temperatures for the α–Al reaction are consistent with the present thermodynamic calculations. Indicating that for the cooling rate of 1.1 K/s the primary crystallization field of Si_2V extends further into the reported phase field of α–Al.

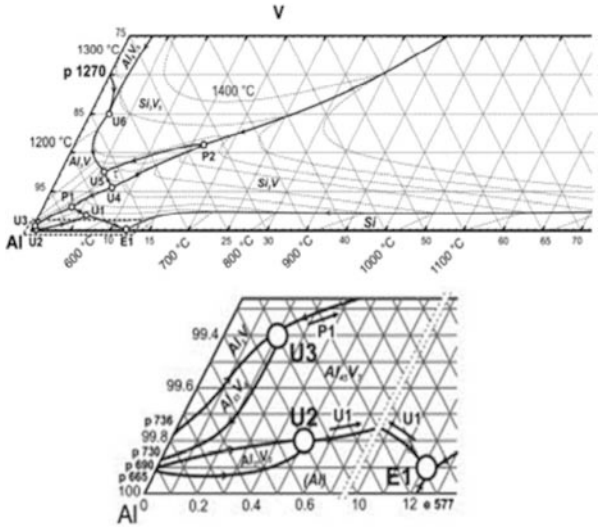

Figure 11 Al-rich part of the liquidus surface projection of the Al-Si-V system with primary crystallization fields and magnification of the Al-rich corner [7].

V additions were found to slightly change plate-like β-Al_5FeSi to more globular structure. Similar findings were reported by Rao [14] for an A319 alloy. It was shown that coarse plate-like Fe-rich phases were modified and formed complex intermetallics with the tendency of possessing equiaxed morphology. Furthermore, from investigations of an AlMgSi alloy it is concluded that V promotes the formation of the α-(AlFeSi) phase [12]. The correlation of Fe and V can be observed by inspection of the binary Fe-V, ternary Al-Fe-Si and quaternary Al-Fe-Si-V system. It becomes apparent that a number of binary and complex Fe and V containing intermetallics can form. These phases are however, not likely to appear in the composition range of an A356 alloy. Others report the substitution of Fe by V in e.g. Fe_3Al [15]. Moreover, almost every Fe_xAl_x phase dissolves some V. Vanadium concentrations in these phases can reach 10 at% even at room temperature, indicating that the increase of V concentration in the β-Al_5FeSi particles is due to incorporation of V into the lattice during the growth. However, the exact mechanism for the V enrichment in β-Al_5FeSi and the morphology change was out of the scope of the present investigations and remains unclear. Here, further studies are needed to understand the effect that V exerts on Fe-rich intermetallic phases.

Conclusion

The influence of V on the microstructure and solidification path of an A356 foundry alloy was investigated by thermal analysis, microscopy and thermodynamic calculations. The concluding remarks of the present study are as follows:

1. Increasing the V concentration from 0.06 wt% to 0.8 wt% results in a shift of nucleation, minimum and growth temperature of α–Al compared to a reference alloy by up to 4.5 K. The undercooling for the α–Al reaction remains unaffected.

2. The addition of V has no apparent influence on the grain size of α–Al.

3. V additions exceeding 0.06 wt% result in the formation of the Si_2V phase with a distinctive polyhedral morphology.

4. Experimentally obtained data for the prediction of the solidification path of the A356 alloy correspond well with thermodynamic calculations using FactSage™ software. The sparsely available phase diagram data in the literature for the Al-Si-V system appears to be incomplete and might be misleading for alloy compositions in the V-lean region.

5. The β-Al_5FeSi phase becomes enriched in V with increasing nominal V additions. It appears as if this is accompanied with changes in the morphology of β-Al_5FeSi.

Acknowledgement

Funding by Hydro Aluminium AS (Norway) is gratefully acknowledged. Thanks are also due to Jan Ove Håvik from Sør-Norge Aluminium AS (Norway) for the generous supply of Al-V master alloy.

References

1. T. Furu et al., "Trace Elements In Aluminium Alloys: Their Origin And Impact On Processability And Product Properties" (Paper presented at the 12th International Conference on Aluminium Alloys, Yokohama, Japan, 2010).
2. G. Jha, F. Cannova and B. Sadler, "Increasing Coke Impurities - Is this really a problem for metal quality?" *Light Metals 2012*, 2012, 1303-1306.
3. J. Grandfield and J.A. Taylor, "The Impact of Rising Ni and V Impurity Levels in Smelter Grade Aluminium and Potential Control Strategies," *Materials Science Forum*, 630 (2009), 129-136.
4. Lennart Bäckerud, Guocai Chai, and Jarmo Tamminen, *Solidification Characteristics of Aluminum Alloys. Vol. 2. Foundry Alloys.* (Des Plaines, IL, AFS, 1990) 127-150.
5. J. Tamminen, *TAW32 - Thermal analysis for Windows*. 2002.
6. V. Raghavan, "Al-Si-V (Aluminum-Silicon-Vanadium)," *Journal of Phase Equilibria and Diffusion*, 32 (01) (2010), 68-71.
7. B. Huber, H.S. Effenberger and K.W. Richter, "Phase equilibria in the Al–Si–V system," *Intermetallics*, 18 (4) (2010), 606-615.
8. E. Gebhardt, G. Joseph, "Über das Dreistoffsystem Aluminium-Silizium-Vanadium," *Zeitschrift für Metallkunde,* 52 (1961), 310–317.
9. Lucio F. Mondolfo, *Aluminum alloys: structure and properties* (London, Butterworths, 1976), 392-394.
10. P. Schumacher et al., "New studies of nucleation mechanisms in aluminium alloys: implications for grain refinement practice," *Materials Science and Technology*, 14 (5) (1998), 394-404.
11. W.M. Edwards et al., "Development of Near-Eutectic Al-Si Casting Alloys for Piston Applications," *Materials Science Forum*, 625 (2002), 396-402.
12. A.H. Maitland and D. Rodriguez, "Vanadium in Aluminium," *Proceedings of the 8th International Light Metals Congress*, 1987, 423-425.
13. P.S. Cooper, M.A. Kearns, and R. Cook, "Effects of residual Transition Metal Impurities on Electrical Conductivity and Grain Refinement of EC Grade Aluminium," *Light Metals 1997,* 1997, 809-814.
14. A.K. Prasada Rao, "Influence of Vanadium on the Microstructure of A319 Alloy," *Transactions of the Indian Institute of Metals*, 64 (4-5) (2011), 447-451.
15. G. Effenberg et al., eds., Landolt-Börnstein, Ternary Alloy Systems Phase Diagrams, Crystallographic and Thermodynamic Data, vol. 11A3 (Springer-Verlag Berlin, Heidelberg, 2005), 1-10.